NASA TECHNICAL NOTE

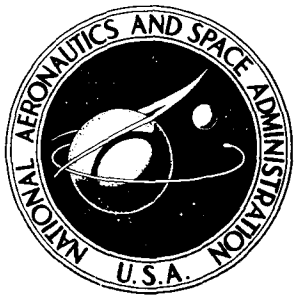

NASA TN D-7568

NASA TN D-7568

DECAY OF FAR FLOW FIELD IN TRAILING VORTICES

by B. S. Baldwin, N. A. Chigier, and Y. S. Sheaffer

Ames Research Center

Moffett Field, Calif. 94035

NATIONAL AERONAUTICS AND SPACE ADMINISTRATION • WASHINGTON, D. C. • FEBRUARY 1974

1. Report No.	2. Government Accession No.	3. Recipient's Catalog No.
D-7568		

4. Title and Subtitle	5. Report Date
DECAY OF FAR FLOW FIELD IN TRAILING VORTICES	January 1974
	6. Performing Organization Code

7. Author(s)	8. Performing Organization Report No.
B. S. Baldwin, N. A. Chigier, and Y. S. Sheaffer	A-5181
	10. Work Unit No.
9. Performing Organization Name and Address	501-06-01-06
Ames Research Center, NASA Moffett Field, Calif. 94035	11. Contract or Grant No.
	13. Type of Report and Period Covered
12. Sponsoring Agency Name and Address	Technical Note
National Aeronautics and Space Administration Washington, D. C. 20546	14. Sponsoring Agency Code

15. Supplementary Notes

16. Abstract

A finite-difference machine code is used in the wake-vortex problem in the quasi-cylindrical boundary-layer approximation. A turbulent-energy model containing new features is developed that accounts for the major effects disclosed by more advanced models in which the parameters are not yet established. Several puzzles that arose in previous theoretical investigations of wake vortices are resolved.

17. Key Words (Suggested by Author(s))	18. Distribution Statement
Trailing Vortices Turbulence Incompressible Flow	Unclassified – Unlimited Cat. 12

19. Security Classif. (of this report)	20. Security Classif. (of this page)	21. No. of Pages	22. Price*
Unclassified	Unclassified	17	$2.75

*For sale by the National Technical Information Service, Springfield, Virginia 22151

NOTATION

a_1	parameter in turbulent energy model (0.15)
C_1	parameter ($0.5C_{\epsilon 1}C_\mu = 0.0643$)
C_2	parameter ($2a_1^{3/2}C_{\epsilon 2} = 0.223$)
C_3	parameter (1.0)
$C_{\epsilon 1}$	parameter (1.43)
$C_{\epsilon 2}$	parameter (1.92)
C_μ	parameter ($4a_1{}^2 = 0.09$)
f	dimensionless kinematic viscosity (eq. (7))
$f_{\max}$	maximum value of f in a given profile
L	mixing length
$PR_\epsilon = 1.3$	Prandtl number in dissipation equation
$PR_\sigma = 1.0$	Prandtl number in energy equation
p	dimensionless pressure (eq. (3))
p_w	approximate dimensionless total pressure (eq. (6))
$\overline{q^2}$	specific (amount per unit mass) time-averaged turbulent fluctuation kinetic energy (times 2)
R,Z	dimensional radial and axial coordinates
r,z	dimensionless radial and axial coordinates $\left(r = \frac{W_\infty R}{\Gamma_\infty},\ z = \frac{W_\infty z}{\Gamma_\infty}\right)$, (e.g., eqs. (1)-(5))
Δr	computational mesh size of r coordinate $\left(= \frac{r_2}{100}\right)$
r_1	dimensionless radius at the position of maximum circumferential velocity (e.g., eqs. (16) and (17))
r_2	dimensionless radius at outer boundary of computational mesh (e.g., eq. (9))
S	dimensional rate of strain

s	dimensionless rate of strain
U, V, W	dimensional radial, circumferential and axial velocity components
u, v, w	dimensionless radial, circumferential, and axial velocity components $\left(\text{e.g., } u = \frac{U}{w_\infty}\right)$, (e.g., eqs. (1) – (5))
W_∞	dimensional free-stream velocity
Δz	variable computational step size
Γ	circulation ($= 2\pi VR$)
Γ_1	circulation at position of maximum circumferential velocity
Γ_∞	circulation at large R
ϵ	specific dissipation of turbulent energy
ν	kinematic viscosity
ν_T	turbulent kinematic viscosity

DECAY OF FAR FLOW FIELD IN TRAILING VORTICES

B. S. Baldwin, N. A. Chigier,* and Y. S. Sheaffer

Ames Research Center

SUMMARY

A finite-difference machine code is used in the wake-vortex problem in the quasi-cylindrical boundary-layer approximation. A turbulent-energy model containing new features is developed that accounts for the major effects disclosed by more advanced models in which the parameters are not yet established. Several puzzles that arose in previous theoretical investigations of wake vortices are resolved.

INTRODUCTION

Methods for reduction of velocities in trailing vortices of large aircraft are of current interest for the purpose of shortening the waiting time between landings at central airports. Procedures for estimating the response of the vortices to stimuli such as air injection or special flap deflections are required. The favorable effect of a special ogee extension at the wing tip has been investigated in wind tunnel experiments by Rorke and Moffitt (ref. 1). It is necessary to determine the effects of this proposal and possibly several others in the far flow field as well as in the near field that can be investigated in wind tunnels. Computer simulation of this problem may eventually produce competitive flexibility.

At the present time definitive simulation of the rate of decay and growth in core size due to turbulent viscosity has not been achieved. A useful review of previous work on this problem and contributions to its solution have been given by Govindaraju and Saffman (ref. 2). Several attempts have been made to simulate the effects of turbulence in wake vortices using integral methods, notably by Kuhn and Nielsen (ref. 3) and Fernandez and Lubard (ref. 4). Additional useful information resulted from these efforts. The wind-tunnel measurements of Hoffmann and Joubert (ref. 5) and Chigier and Corsiglia (ref. 6) have been used extensively and have contributed to the present knowledge of turbulent wake vortices. A preliminary calculation of the flow in an isolated vortex has been made by Donaldson (ref. 7) based on a sophisticated turbulence theory. The method of invariant modeling employed should be useful in the development of future turbulence theories.

Investigators at the Imperial College in London (e.g., ref. 8) have developed turbulence models in which the length scale is governed by an additional differential equation in lieu of assignment of a length scale as in Donaldson's model. Application of this concept to turbulent wake vortices in the present paper leads to a significant departure from Donaldson's prediction of the rate of decay of

---

*Senior Lecturer, University of Sheffield, England.

such vortices. An effect of suppression of turbulence due to curvature of the flow contained in Donaldson's model, but not in that of Launder and others, also plays an important role. A method for including these two effects in an extension of Prandtl's turbulent energy model (ref. 9) is developed in the present paper. The relatively slow rate of decay of turbulent wake vortices that has been observed in flight experiments (ref. 10) is thereby explained. The approach to self-similar solutions predicted in earlier investigations by Donaldson (ref. 7) and Baldwin and others (ref. 11) does not occur when both of the above effects are considered.

THEORY

Quasi-Cylindrical Flow

The basic equations in the boundary-layer approximation are taken from Lilley and Chigier (ref. 12). Attention has been confined to incompressible flow in this paper and the equations reduced to a nondimensional form through division of the velocities by the free-stream velocity W_∞, division of the pressure by $\rho_\infty W_\infty^2$, and multiplication of the axial and radial coordinates by the factor W_∞/Γ_∞. The resulting equations in a nondimensional form suitable for finite difference solution are

$$\frac{\partial p_w}{\partial z} = \left(-u\,\frac{\partial w}{\partial r} + \frac{1}{r}\,\frac{\partial}{\partial r}\,fr\,\frac{\partial w}{\partial r}\right) \tag{1}$$

$$\frac{\partial v}{\partial z} = \frac{1}{w}\left[-u\left(\frac{\partial v}{\partial r} + \frac{v}{r}\right) + \frac{1}{r^2}\,\frac{\partial}{\partial r}\,fr^3\,\frac{\partial}{\partial r}\,\frac{v}{r}\right] \tag{2}$$

$$\frac{\partial p}{\partial r} = \frac{v^2}{r} \tag{3}$$

$$w = \sqrt{2(p_w - p)} \tag{4}$$

$$\frac{\partial ru}{\partial r} = -r\,\frac{\partial w}{\partial z} \tag{5}$$

where

$$p_w = p + (1/2)\,w^2 \tag{6}$$

$$f = (\nu_T/\Gamma_\infty) + (\nu/\Gamma_\infty) \tag{7}$$

The turbulent viscosity coefficient ν_T is determined from a turbulence model to be discussed. The boundary conditions are

$$u(r_2,z) = 0 \tag{8}$$

$$v(r_2,z) = 1/2\pi r_2 \tag{9}$$

$$w(r_2,z) = 1 \tag{10}$$

$$p(r_2,z) = 0 \tag{10a}$$

where r_2 is a radius large compared to the size of the core (r_1). At the center of the core

$$u(0,z) = 0 \tag{11}$$

$$v(0,z) = 0 \tag{12}$$

The initial conditions are

$$u(r,z_0) = 0 \tag{13}$$

$$v(r,z_0) = f_v(r/r_1) \tag{14}$$

$$w(r,z_0) = 1 + f_w(r/r_1) \tag{15}$$

where r_1 is the radius at which the circumferential velocity is a maximum.

Turbulence Model

Since detailed experimental information on the flow in turbulent vortices is not yet available, methods that depend on evaluation of parameters from the particular experiment at hand cannot be used. Instead, a complete model is needed that bears an approximate relationship to the exact flow in a manner analogous, for example, to the relationship between simple kinetic theory and the rigorous kinetic theory of gases. It has been shown by Launder and others (ref. 8) that Prandtl's 1945 turbulent energy model (ref. 9) works reasonably well in axisymmetric wakes. The basic equation can be written (in the notation of A. Townsend, ref. 13)

$$\frac{D(1/2)\overline{q^2}}{Dt} = \frac{1}{PR_Q}\,\vec{\nabla}\cdot\nu_T\vec{\nabla}\left(\frac{1}{2}\overline{q^2}\right) + \sqrt{a_1}\;LS^2\sqrt{\overline{q^2}} - \frac{a_1^{3/2}(\overline{q^2})^{3/2}}{L} + F \tag{16}$$

where F is an additional term developed in this paper. The kinematic-turbulent-viscosity coefficient ν_T and local shear are given by

$$\nu_T = \sqrt{a_1}\,L\sqrt{\overline{q^2}} \tag{17}$$

$$S = \sqrt{\left(\frac{\partial W}{\partial R}\right)^2 + \left(R\frac{\partial}{\partial R}\frac{V}{R}\right)^2} \tag{18}$$

For later discussion it is worthwhile to consider the production term of equation (16) in more detail. Since

$$\left(R\frac{\partial}{\partial R}\frac{V}{R}\right)^2 = \left(\frac{\partial V}{\partial R}\right)^2 + 3\frac{V^2}{R^2} - 2\frac{V}{R^2}\frac{\partial VR}{\partial R} \tag{19}$$

the production term can be written

$$\sqrt{a_1}LS^2\sqrt{\overline{q^2}} = \sqrt{a_1}\left[\left(\frac{\partial W}{\partial R}\right)^2 + \left(\frac{\partial V}{\partial R}\right)^2 + 3\frac{V^2}{R^2} - 2\frac{V}{R^2}\frac{\partial(VR)}{\partial R}\right]L\sqrt{\overline{q^2}} \tag{20}$$

In axisymmetric wakes, the mixing length L is assigned a uniform value that is taken to be a constant fraction of the width of the wake. However, Launder and others (ref. 8) have developed an additional equation from which the mixing length can be computed rather than assigning its value (again in Townsend's notation)

$$\frac{D\epsilon}{Dt} = \frac{1}{PR_\epsilon}\vec{\nabla}\cdot\nu_T\vec{\nabla}\epsilon + C_1\overline{q^2}S^2 - \frac{C_2\sqrt{\overline{q^2}\epsilon}}{L} \tag{21}$$

and

$$L = a_1^{3/2}(\overline{q^2})^{3/2}/\epsilon \tag{22}$$

Launder and others (ref. 8) and Hanjalic and Launder (ref. 14) have shown that computation of the mixing length in this manner leads to improvement of comparisons with measurements in a variety of turbulent free shear flows as well as boundary layers.

The foregoing turbulence model does not apply to turbulent vortices because it does not account for suppression of turbulence due to curvature of the mean flow that has been disclosed by more advanced models such as that of Donaldson (ref. 7). This effect is illustrated in figure 1, which represents a rotating flow in cross section. The Rayleigh stability criterion indicates that if the product VR decreases in the outward direction, the flow is unstable against disturbances that would interchange fluid between inner and outer regions. Conversely, if the product VR increases in the outward direction, there is a damping effect on turbulent eddies produced by the shearing motion. This concept can be made quantitative by finding the energy per unit mass of fluid required to interchange fluid between the inner and outer annuli, while retaining an unchanged angular momentum of the fluid transferred

$$\Delta\frac{1}{2}\overline{q^2} = \frac{1}{2}\Delta(VR)^2 \times \Delta\frac{1}{R^2} \approx -2\frac{V}{R^2}\frac{\partial VR}{\partial R}L^2$$

The rate of transfer of fluid by an eddy of size L and velocity $\overline{q^2}$ is approximated by

$$\frac{1}{m}\frac{dm}{dt} \approx \frac{\sqrt{\overline{q^2}}}{L}$$

These relations can be combined to obtain an additional term to be included in the turbulent energy equation (18). The new turbulence suppression term is

$$F = -2\frac{V}{R^2}\frac{\partial(VR)}{\partial R} L\sqrt{q^2}\, C_3 \tag{23}$$

This relation applies more generally to flows with curvature if R is taken to be the local radius of curvature of streamlines. Present information does not permit determination of a better value of the magnitude of this term than that resulting from the above derivation ($C_3 = 1.0$).

It is interesting to note that the suppression term is of the same form and same sign as a term arising from the shear that is already present in Prandtl's energy equation, namely, the last term in equation (20). One might wonder whether the curvature suppression effect discussed above is already included in Prandtl's model. However, as can be seen in equation (18), the shear contribution to the production of turbulence must always be positive because it consists of a sum of squared quantities. It seems clear that Rayleigh instability should enhance the growth of turbulence and an opposite stabilizing condition of the mean flow should be capable of stopping the growth entirely, as in the suppression of turbulence due to buoyancy forces (e.g., ref. 15). We therefore conclude that the term given in equation (23) should be included again even if it does already appear in the production term due to a different mechanism (shearing motion rather than curvature of the mean flow).

It may be possible to simulate the suppression of turbulence by making the length L smaller so that the effect of turbulent mixing is reduced and the rate of production due to shear decreased. An improvement in the agreement of calculations with measurements in curved boundary layers was achieved in this manner by Bradshaw (ref. 16). In near-equilibrium situations it may be possible to relate that method to the present one. However, the mechanism by which such an effect would enter the dissipation equation (eq. (19)) is not clear to the present authors, whereas the origin of the energy suppression term (eq. (23)) seems relatively obvious.

As mentioned earlier, the turbulence model of Donaldson (ref. 7) contains a curvature suppression effect that enters through the tensor formalism used in the method of invariant modeling. Ultimately, such an approach may be more satisfactory than that employed here. We have been unable to relate our method to that of Donaldson and have not been convinced that his treatment of the effect is yet in final form. For the present, we prefer simple physical reasoning applied to the special type of flow under consideration in which the origin of the effect seems understandable.

The nondimensional forms of the energy and dissipation equations used in the finite-difference calculations are

$$\frac{\partial\kappa}{\partial z} = \frac{1}{w}\left[-u\frac{\partial\kappa}{\partial r} + \frac{C_\mu}{PR_Q}\frac{1}{r}\frac{\partial}{\partial r}\left(r\ell\sqrt{\kappa}\frac{\partial\kappa}{\partial r}\right) + C_\mu\sqrt{\kappa}\ell S^2 - \frac{\kappa^{3/2}}{\ell} - 2^{3/2}\, C_3\frac{v}{r^2}\frac{\partial(vr)}{\partial r}\ell\sqrt{\kappa}\right] \tag{24}$$

$$\frac{\partial \xi}{\partial z} = \frac{1}{w}\left[-u\frac{\partial \xi}{\partial r} + \frac{C_\mu}{PR_\epsilon}\frac{1}{r}\frac{\partial}{\partial r}\left(r\ell\sqrt{\kappa}\frac{\partial \xi}{\partial r}\right) + C_{\epsilon 1}C_\mu \kappa s^2 - C_{\epsilon 2}\frac{\xi^{4/3}}{\ell^{2/3}}\right] \tag{25}$$

where

$$\kappa = \overline{q^2}/2W_\infty^2 \tag{26}$$

$$\xi = (\Gamma_\infty/W_\infty^4)\epsilon \tag{27}$$

The dimensionless local shear s and length ℓ are given by

$$s = \sqrt{\left(\frac{\partial w}{\partial r}\right)^2 + \left(r\frac{\partial}{\partial r}\frac{v}{r}\right)^2} \tag{28}$$

$$\ell = \kappa^{3/2}/\xi \tag{29}$$

The numerical values of the constants (taken from Launder *et al.*, ref. 8) are given in the list of notation. The dimensionless turbulent viscosity coefficient is

$$(\nu_T/\Gamma_\infty) = C_\mu\sqrt{\kappa}\ell \tag{30}$$

Computational Procedure

A machine code was developed for finite-difference solution of the foregoing relations according to the explicit predictor-corrector method of MacCormack (ref. 17). Equations (1), (2), (24), and (25) are stepped forward in z to obtain values of p_w, v, κ, and ξ. At each step, equation (3) is integrated by quadrature to optain p. Equation (4) can then be used to evaluate w. The derivative $\partial w/\partial z$ is computed by finite-difference and equation (5) is integrated by quadrature to obtain u. In the explicit method used to step forward in z, all auxiliary quantities are evaluated in terms of the independent and primary dependent variables by means of the remaining formulas. One hundred equally spaced mesh points are used for the radial coordinate r. The step size of the axial coordinate z is dictated by the requirements of numerical stability. Instabilities arising from the last term in equation (1) are dominant according to an analysis based on the methods of Lomax and Bailey (ref. 18). A workable stability criterion was found to be

$$\Delta z < 0.3(\Delta r)^2/f_{\max} \tag{31}$$

RESULTS

For isotropic shear flows, the simplified turbulence model described accounts for the major effects disclosed by more advanced models in which the parameters are not yet established. It therefore applies to turbulent vortices with small axial velocities and can be expected to lead to

realistic predictions of changes taking place in the far flow field of wake vortices. We have made finite difference calculations based on this model in the quasi-cylindrical approximation. Since information on the initial values of the axial and radial velocities is unavailable, these velocities have been set equal to zero. Thus calculations in this report correspond to an isolated vortex extending from $-\infty$ to $+\infty$ through the transformation $t = Z/W_\infty$.

In the middle of figure 2 are shown computed circulation profiles with free-stream velocity W_∞, circulation at large radius Γ_∞, and wing chord c assigned values corresponding to the Cherokee flight data of McCormick, Tangler, and Sherrieb (ref. 10). The calculations were started at $z = 0$ with an initial circulation profile corresponding to that of a self-similar laminar vortex (Lamb vortex). As shown in the profile at 34.5 chord lengths behind the wing, an overshoot develops in the circulation and moves outward. In the inner regions where the circulation rises steeply, the curvature suppression results in reduced mixing so that changes take place more slowly than in the outer regions. The corresponding velocity profiles appear at the top of figure 2.

At the bottom of figure 2, a typical turbulent intensity profile at a downstream station 34.5 chord lengths behind the wing is shown. The solid curve represents the computed turbulent intensity and the dashed curve indicates the equilibrium values that would be present if the production and dissipation terms in the turbulent energy equation (eq. (18)) were balanced to zero. The equilibrium values are large at a radius of 40 in. (1.016 m) because the gradient of circulation is negative in that region as can be seen in the middle curves of figure 2. This negative gradient leads to an enhancement rather than suppression of turbulence as indicated by equations (18) and (23). However, there is a lag of the actual turbulence below the equilibrium values. The turbulence is weak inside the radius of maximum velocity so that relatively slow changes in velocity occur there. The local peak in turbulent intensity near the radius of maximum velocity can be attributed to changes outside this radius which enhance the local shear leading to production of turbulence.

Figure 3 contains profiles of the computed mixing length at three axial stations. The calculation was started with a uniform mixing length at $z = 0$. However, the values quickly change within 10 chord lengths and become highly nonuniform across the profile. In the region of circulation overshoot where the turbulence is enhanced, the eddies become quite large. The eddy size quickly decreases to very small values inside the radius of maximum velocity where the turbulent intensity is also small due to curvature suppression. In figure 4 are shown turbulent viscosity profiles. These results indicate that there is considerable turbulent mixing in the outer part of the vortex, but very little near the point of maximum velocity.

Figure 5 contains estimates of the decay of maximum circumferential velocity according to several turbulence models. The circles represent the flight data of McCormick and others (ref. 10). The lower curve indicates a typical result from previous investigations (refs. 4 and 11) in which the suppression of turbulence due to curvature of the flow is not taken into account. In the middle curve, this effect was included but the mixing length was taken to be a constant fraction of the radius of maximum velocity. In that case the calculation indicates appreciable encroachment of turbulence into the core by diffusion as in Donaldson's calculation (ref. 7). However, if the variable mixing length is accounted for by integration of equation (21), such diffusion is inhibited by the very small mixing length that exists near the radius of maximum velocity. The top curve is based on the complete model with all large effects taken into account.

There are several possible explanations for the discrepancy between the upper curve and the flight data represented by the circles. Calculations based on different initial circulation profiles may lead to better agreement. Also, it is known that the level of ambient atmospheric turbulence affects the rate of decay. Rapid decays occur in rough air, possibly due to time dependent distortions of the circulation profiles introduced by the buffeting. In calm air, slow decays take place that would be in better agreement with calculations not including such effects. The important point is that the present simplified turbulence model predicts slow decays, in contrast to previous results that were in gross disagreement with flight data. This model indicates that the level of turbulence inside the radius of maximum velocity is much lower than previously supposed. The initial roll up is more nearly inviscid than many of us believed, particularly in the inner regions. Two basic mechanisms are responsible for this phenomenon. One is the suppression of turbulence due to curvature of the flow (eq. (23)). The other is the variable mixing length (fig. 3) which becomes small near the radius of maximum velocity, thereby inhibiting the inward diffusion of turbulence. These effects lead to small turbulent mixing in the inner regions of the vortex, so that the approach to self-similar solutions noted in previous investigations (refs. 7 and 11) does not occur.

Ames Research Center
National Aeronautics and Space Administration
Moffett Field, Calif. 94035, October 12, 1973

REFERENCES

1. Rorke, J. B.; Moffitt, R. C.; and Ward, J. F.: Wind Tunnel Simulation of Full Scale Vortices. Presented at the 28th Annual National Forum of the American Helicopter Society, Preprint No. 623, Washington, D.C., May 1972.

2. Govindaraju, S. P.; and Saffman, P. G.: Flow in a Turbulent Trailing Vortex. Phys. Fluids, vol. 14, no. 10, Oct. 1971, pp. 2074-2080.

3. Kuhn, G. D.; and Nielsen, J. N.: Analytical Studies of Aircraft Trailing Vortices. AIAA Paper 72-42, Jan. 1972.

4. Fernandez, F. L.; and Lubard, S. C.: Turbulent Vortex Wakes and Jets. AIAA Paper 71-615, June 1971.

5. Hoffmann, E. R.; and Joubert, P. N.: Turbulent Line Vortices. J. Fluid Mech., vol. 16, pt. 3, July 1963, pp. 395-411.

6. Chigier, N. A.; and Corsiglia, N. A.: Wind-Tunnel Test Data for Wing Trailing Vortex Flow Survey. NASA TM X-62,148, 1972.

7. Donaldson, C. duP.: Calculations of Turbulent Shear Flows for Atmospheric and Vortex Motions. AIAA Paper 71-217, Jan. 1971.

8. Launder, B. E.; Morse, A.; Rodi, W.; and Spalding, D. B.: The Prediction of Free Shear Flows – A Comparison of the Performance of Six Turbulence Models. Paper presented at the NASA Conference on Free Shear Flows, vol. 1, NASA SP-321, 1973, pp. 361-426.

9. Prandtl, L.: Über ein neues Formelsystem für die Ausgebildeten Turbulenz. Nachr. Akad. Wiss. Göttingen, 1945, pp. 6-19.

10. McCormick, B.W.; Tangler, J. L.; and Sherrieb, H. E.: Structure of Trailing Vortices. J. Aircraft, vol. 5, no. 3, May-June 1968, pp. 260-267.

11. Baldwin, B. S.; Chigier, N. A.; and Sheaffer, Y. S.: Prediction of Far Flow Field in Trailing Vortices. AIAA Paper 72-989, Sept. 1972.

12. Lilley, D. G.; and Chigier, N. A.: Nonisotropic Turbulent Stress Distribution in Swirling Flows from Mean Value Distributions. International J. Heat and Mass Transfer, vol. 14, no. 4, April 1971, pp. 573-585.

13. Townsend, A. A.: Equilibrium Layers and Wall Turbulence. J. Fluid Mech., vol. 11, pt 1, August 1961, pp. 97-120.

14. Hanjalic, K.; and Launder, B. E.: A Reynolds Stress Model of Turbulence and its Application to Thin Shear Flows. J. Fluid Mech., vol. 52, pt. 4, April 25, 1972, pp. 609-638.

15. Townsend, A. A.: Turbulent Flow in a Stably Stratified Atmosphere. J. Fluid Mech., vol. 3, pt. 4, Jan. 1958, pp. 361-372.

16. Bradshaw, P.: Analogy Between Streamline Curvature and Buoyance in Turbulent Shear Flow. J. Fluid Mech., vol. 36, pt. 1, March 27, 1969, pp. 177-191.

17. MacCormack, R. W.: The Effect of Viscosity in Hypervelocity Impact Cratering. AIAA Paper 69-354, April 1969.

18. Lomax, Harvard; and Bailey, R. F.: Computational Method for Calculating Convection in a Rotating Tank. Chapter 3 in NASA TR R-386, Convection in the Tanks of a Rotating Spacecraft, by Computational Fluid Dynamics Branch at Ames Research Center, 1972, pp. 39-59.

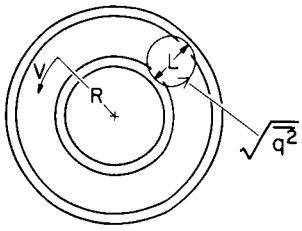

Figure 1.– Rotating flow in cross section.

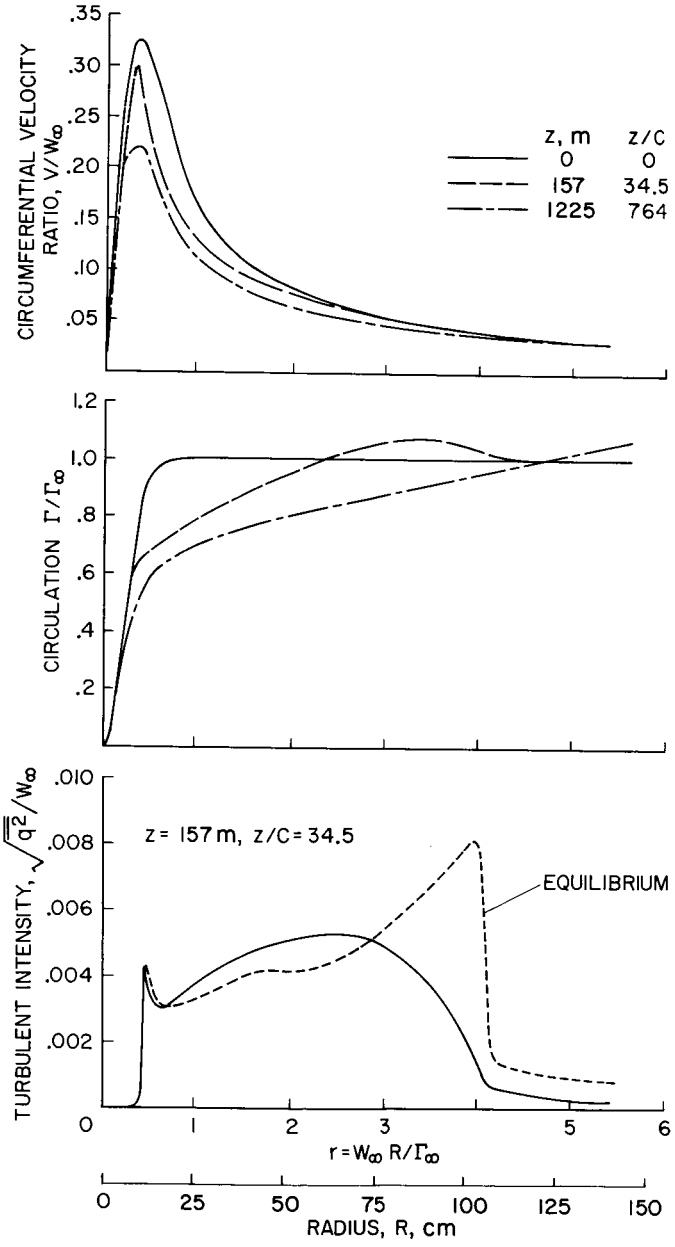

Figure 2.– Profiles in wake vortex (W_∞ = 132 ft/sec (40.2 m/sec), Γ_∞ = 112 ft^2/sec (10.4 m^2/sec), c = 5.26 ft (1.60 m)).

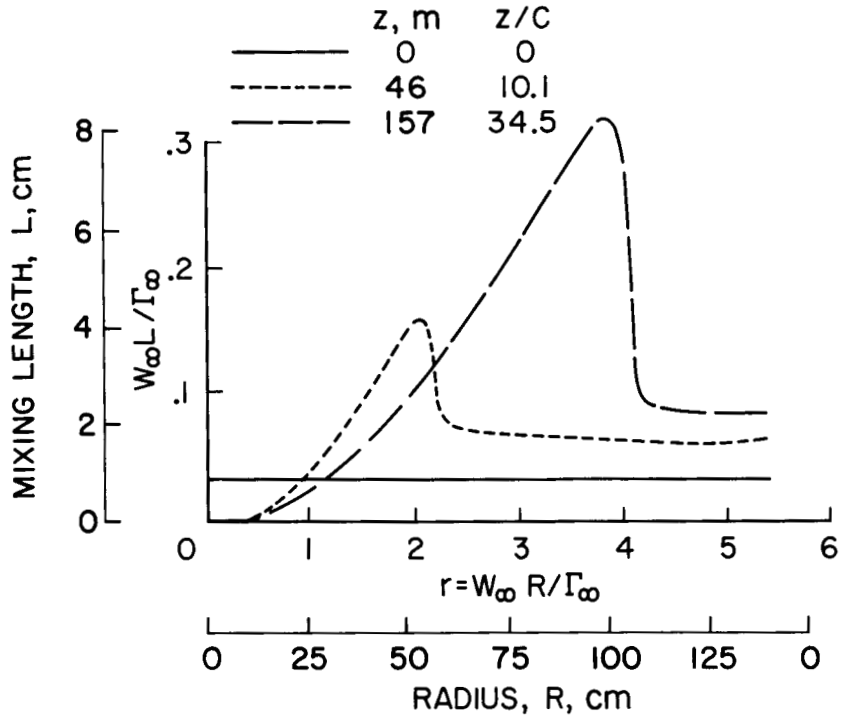

Figure 3.– Mixing length (W_∞ = 132 ft/sec (40.2 m/sec), Γ_∞ = 112 ft^2/sec (10.4 m^2/sec), c = 5.26 ft (1.60 m)).

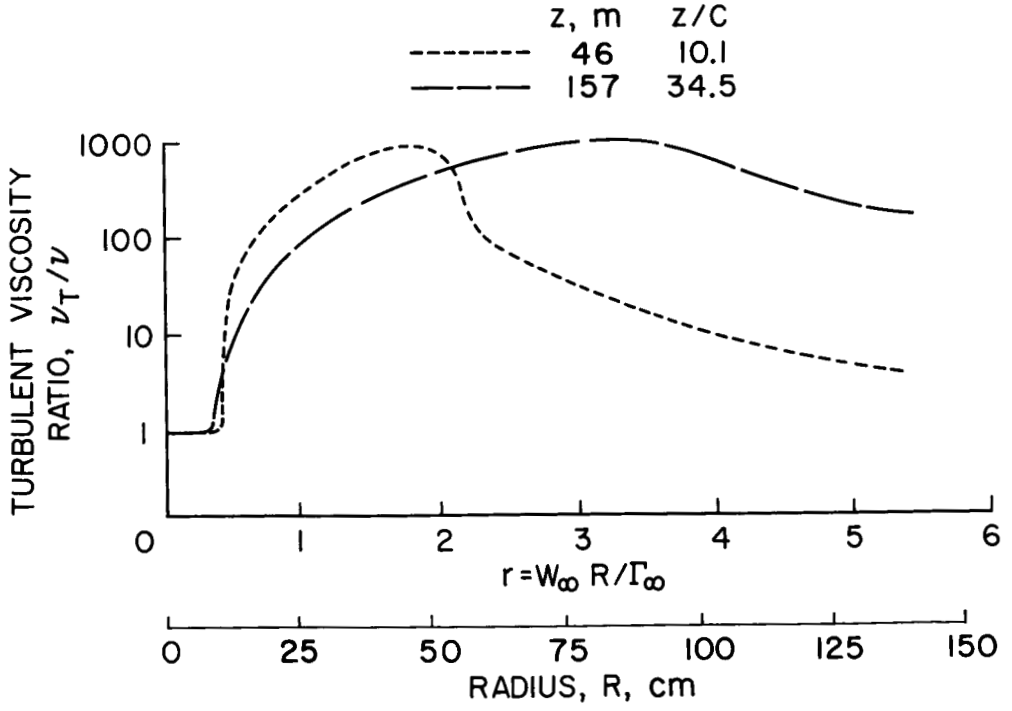

Figure 4.– Turbulent viscosity profiles (W_∞ = 132 ft/sec (40.2 m/sec), Γ_∞ = 112 ft^2/sec (10.4 m^2/sec), c = 5.26 ft (1.60 m)).

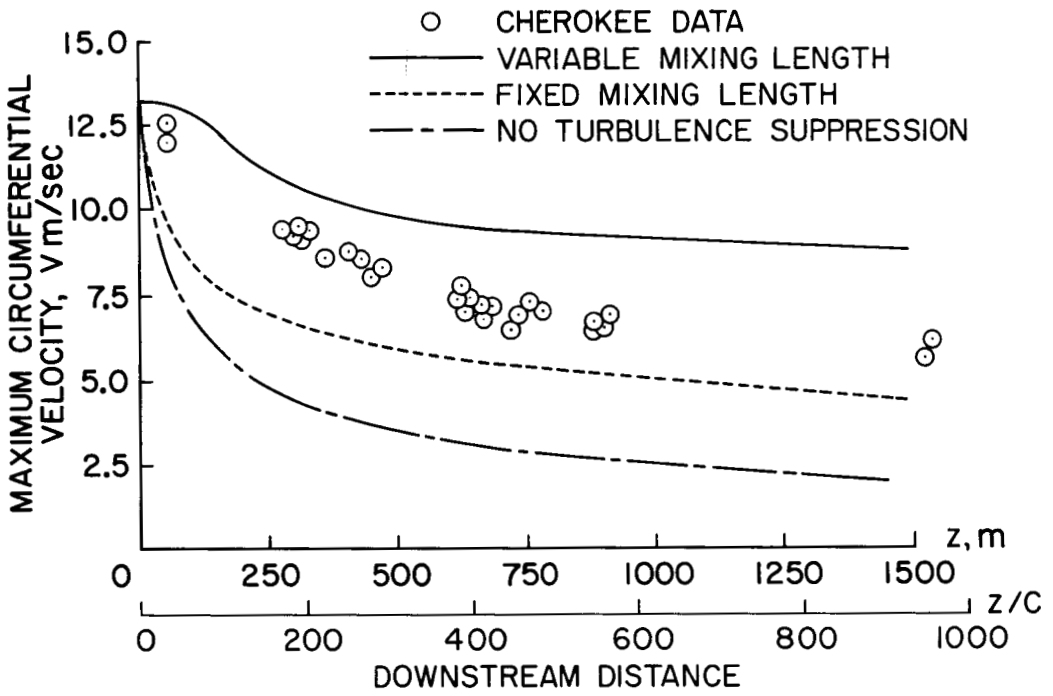

Figure 5.– Decay of wake vortex (W_∞ = 132 ft/sec (40.2 m/sec), Γ_∞ = 112 ft^2/sec (10.4 m^2/sec), c = 5.26 ft (1.60 m)).